Electronic Supplementary Material (ESI) for CrystEngComm.

Novel co-crystals with π-hole interactions between iodide anions and quinoid rings involving charge transfer

Supplement

Valentina Milašinović and Krešimir Molčanov

Ruđer Bošković Institute, Bijenička 54, Zagreb HR-10000, Croatia

e-mail: kmolcano@irb.hr

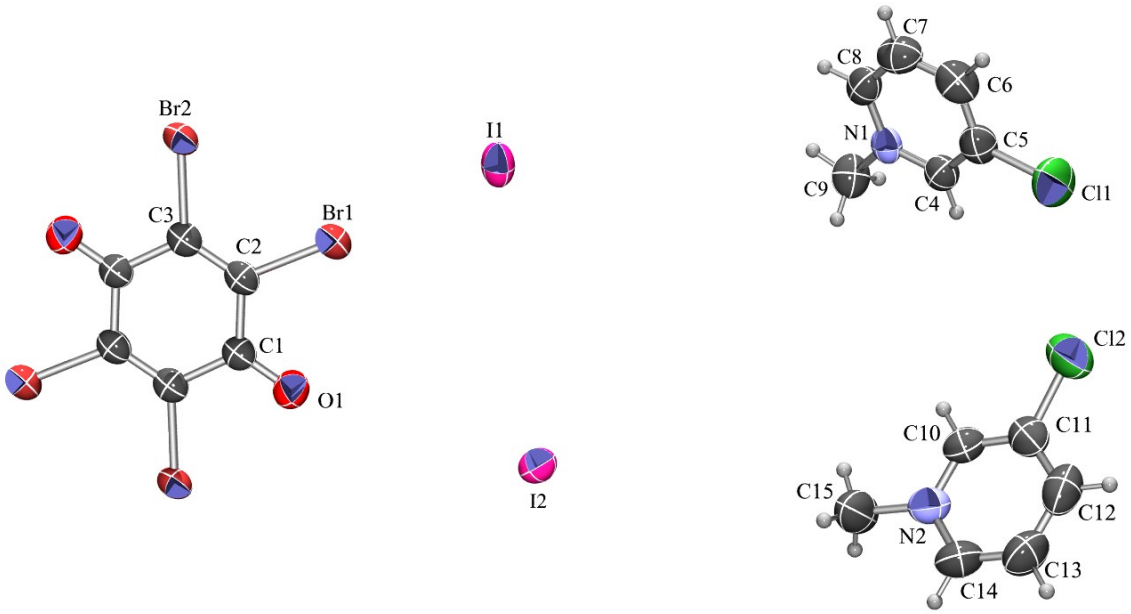

Figure S1 ORTEP-3 drawing of asymmetric unit of **1** with the atom numbering scheme. Displacement ellipsoids are drawn for the probability of 50% and hydrogen atoms are shown as spheres of arbitrary radii.

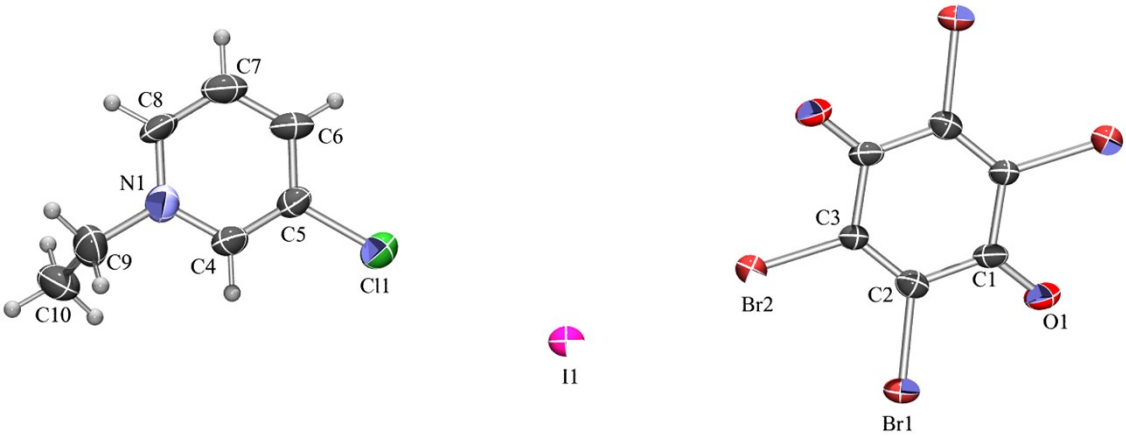

Figure S2 ORTEP-3 drawing of asymmetric unit of **2** with the atom numbering scheme. Displacement ellipsoids are drawn for the probability of 50% and hydrogen atoms are shown as spheres of arbitrary radii.

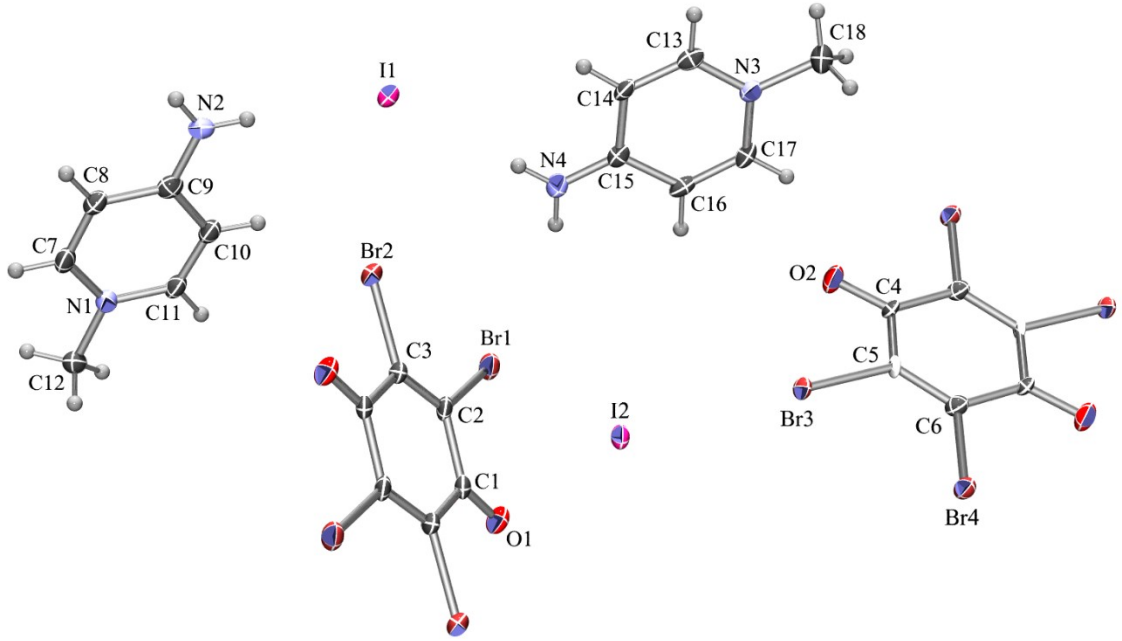

Figure S3 ORTEP drawings of asymmetric unit of **3** with the atom numbering schemes. Displacement ellipsoids are drawn for the probability of 50% and hydrogen atoms are shown as spheres of arbitrary radii.

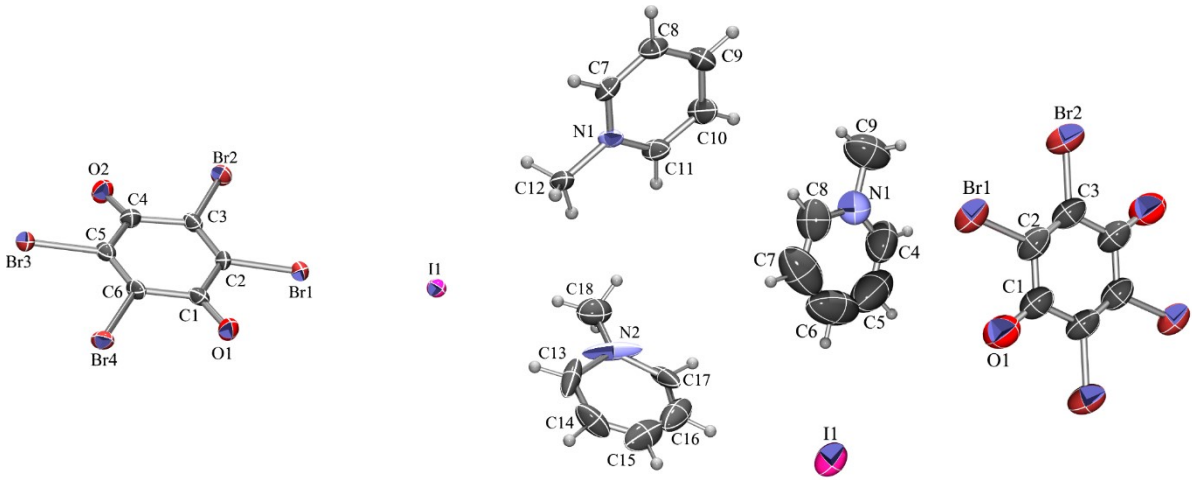

a) b)

Figure S4 ORTEP drawing of asymmetric unit of **4** at: a) 100 K and b) room temperature. Displacement ellipsoids are drawn for the probability of 50% and hydrogen atoms are shown as spheres of arbitrary radii.

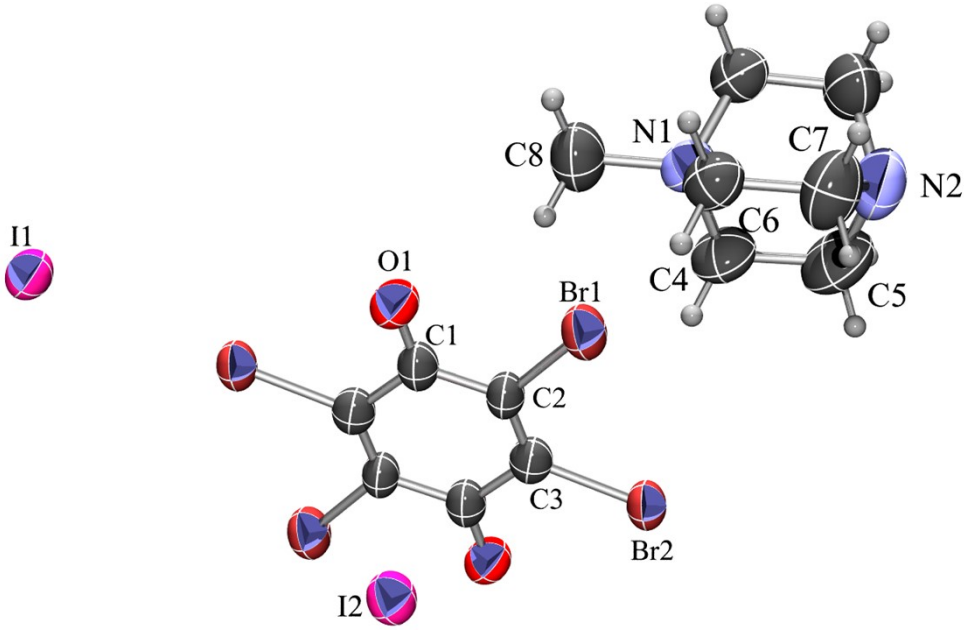

Figure S5 ORTEP drawing of asymmetric unit of **5** with the atom numbering scheme. Displacement ellipsoids are drawn for the probability of 50% and hydrogen atoms are shown as spheres of arbitrary radii.

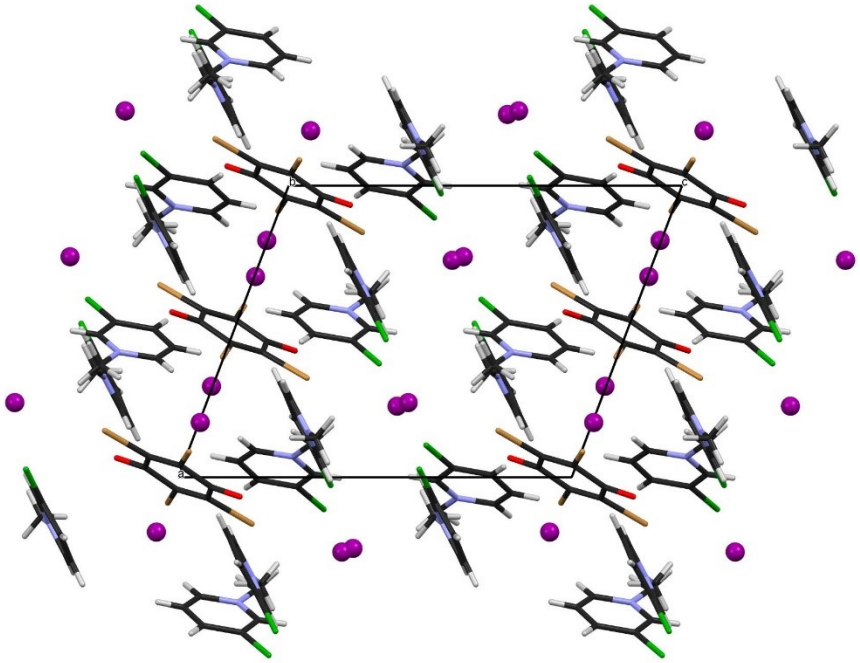

Figure S6 Crystal packing of **1**. Iodide ions are shown as spheres of arbitrary radii.

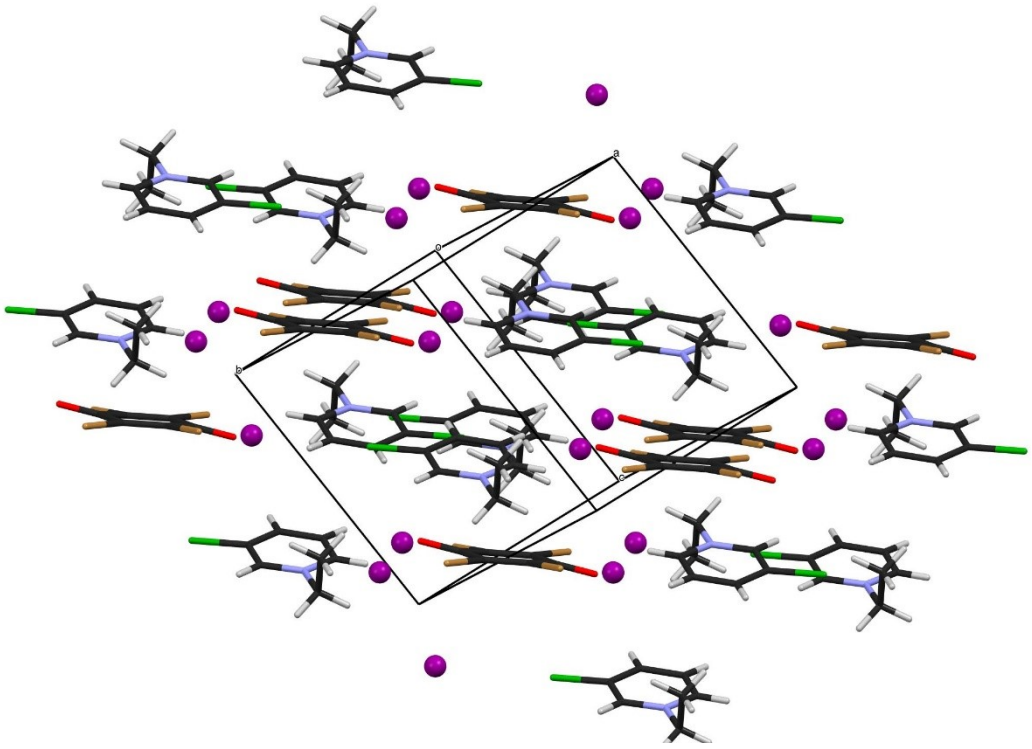

Figure S7 Crystal packing of **2**. Iodide ions are shown as spheres of arbitrary radii.

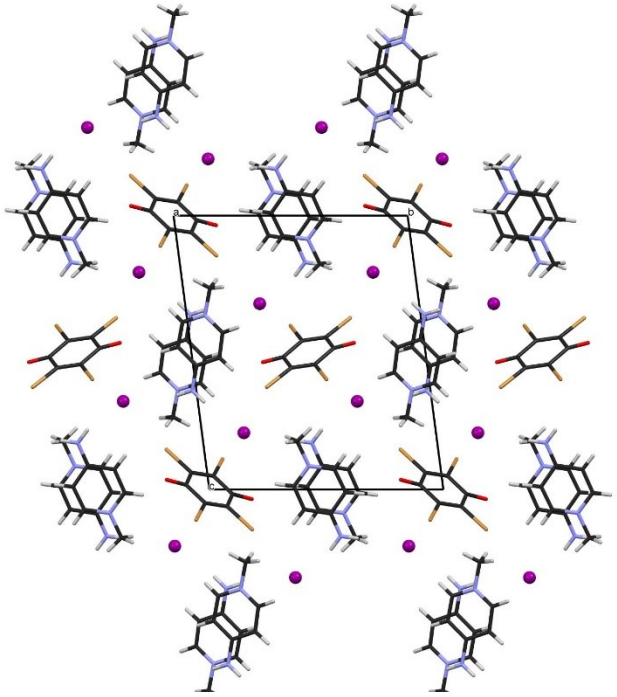

Figure S8 Crystal packing of **3**. Iodide ions are shown as spheres of arbitrary radii.

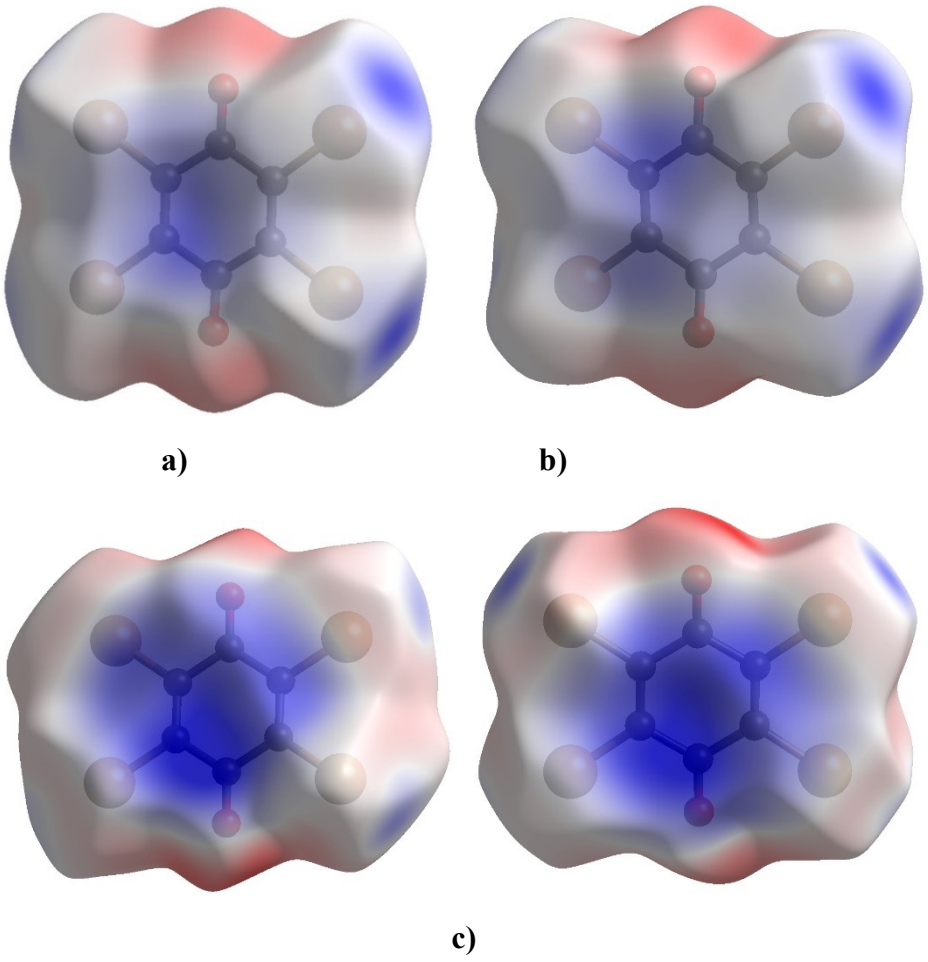

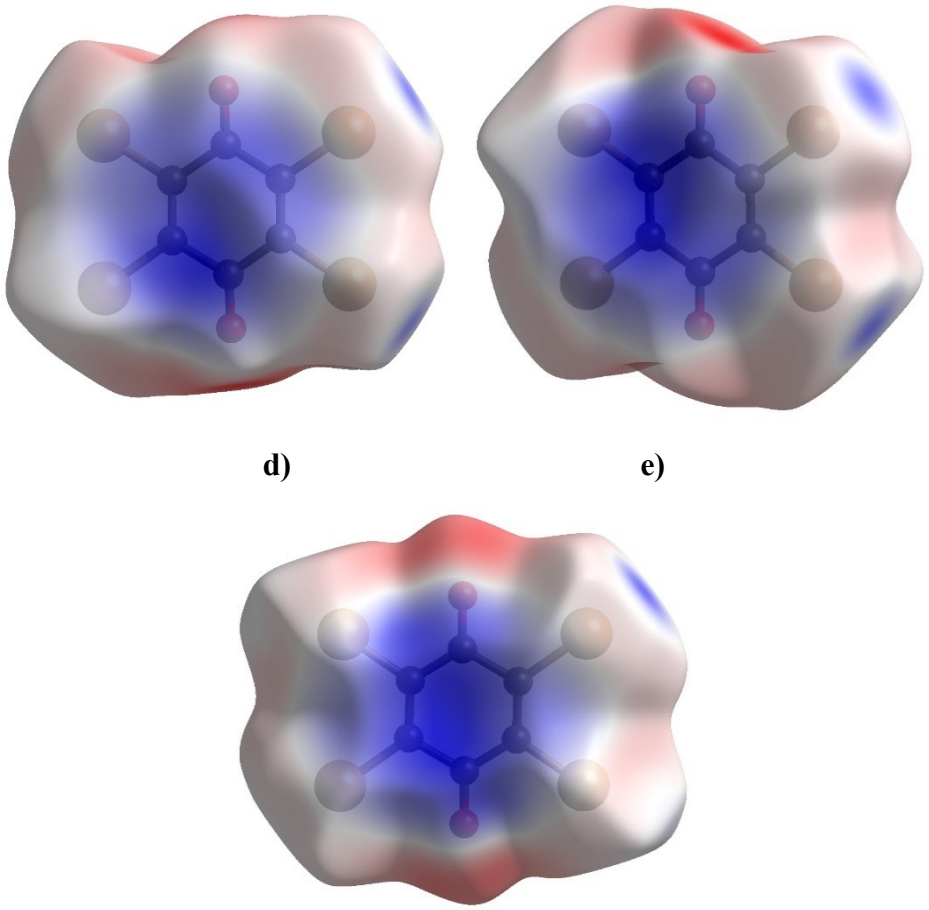

Figure S9 The electrostatic potential plotted onto a Hirshfeld surface of Br_4Q for a) **1**, b) **2**, c) two symmetry-independent quinones in **3**, d) **4** at 100 K, e) **4** at RT and f) **5**.

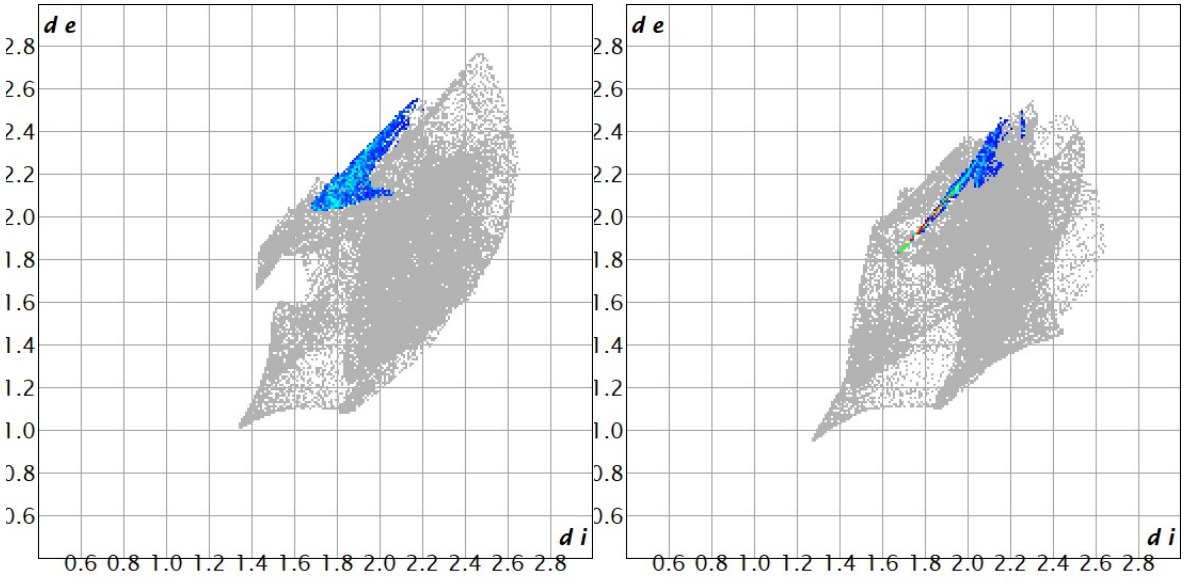

a) **b)**

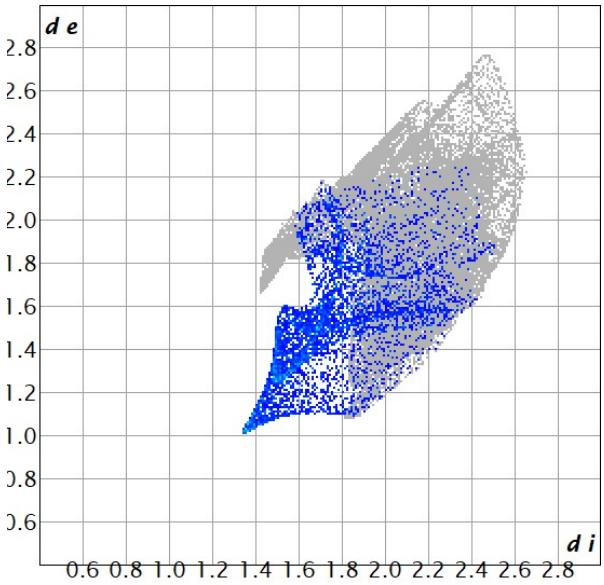

c)

Figure S10 Fingerprint plots of intermolecular contacts in **1** for a) C···I, b) Br···I and c) O···H.

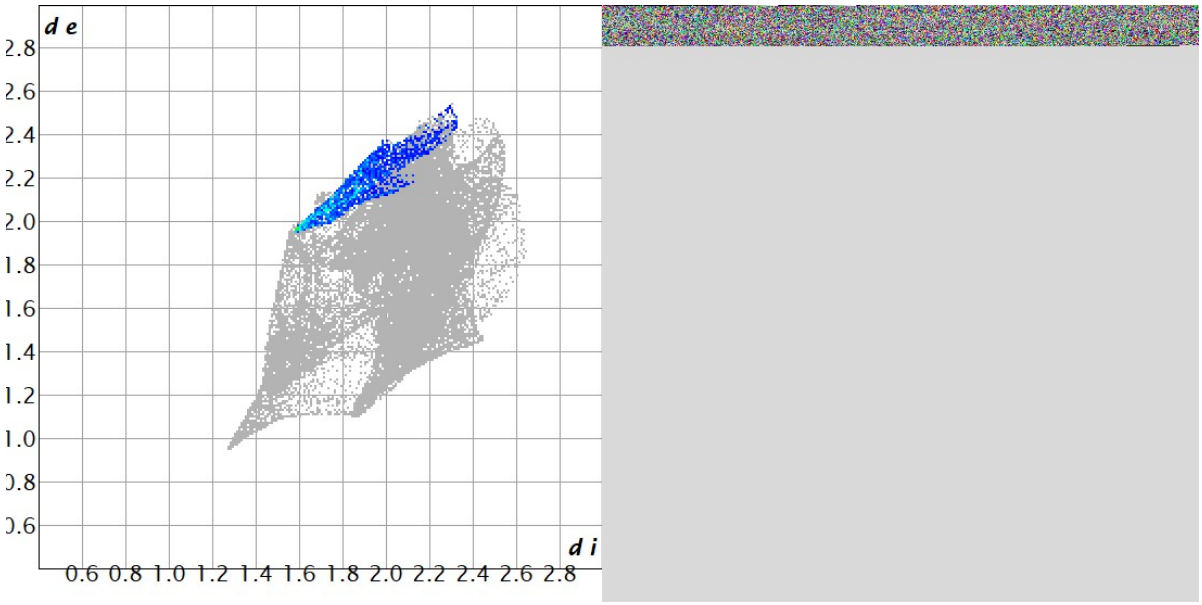

a) **b)**

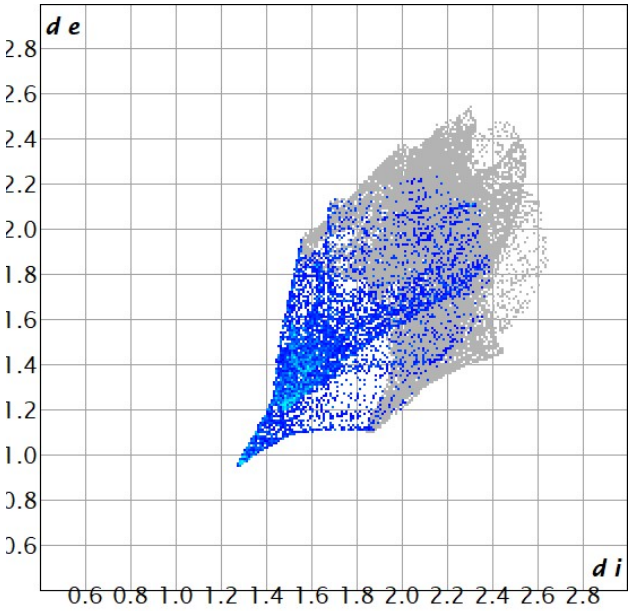

c)

Figure S11 Fingerprint plots of intermolecular contacts in **2** for a) C···I, b) Br···I and c) O···H.

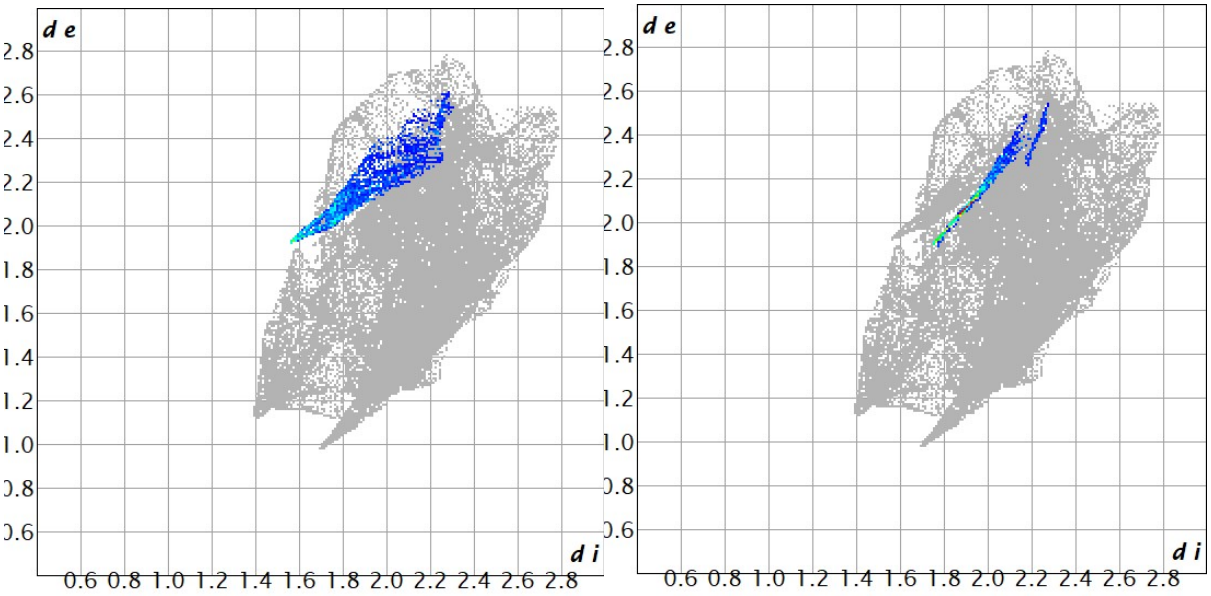

a) **b)**

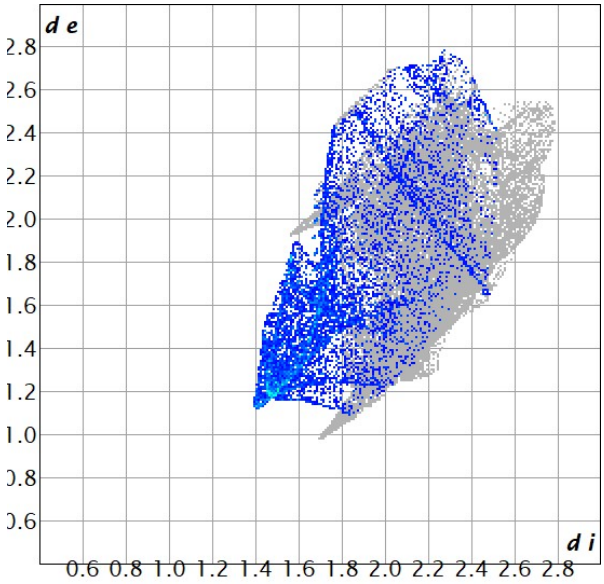

c)

Figure S12 Fingerprint plots of intermolecular contacts in **3** (molecule 1) for a) C···I, b) Br···I and c) O···H.

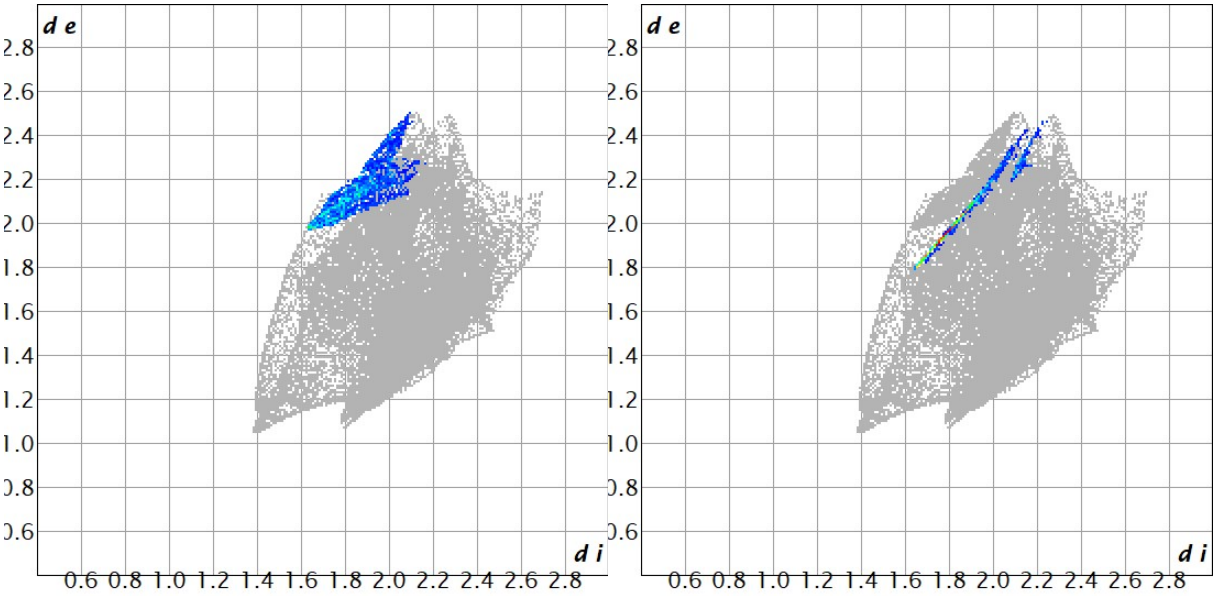

a) **b)**

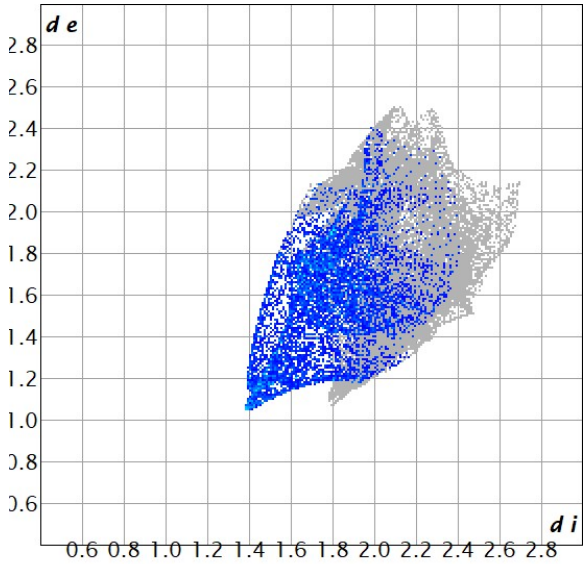

c)

Figure S13 Fingerprint plots of intermolecular contacts in **3** (molecule 2) for a) C···I, b) Br···I and c) O···H.

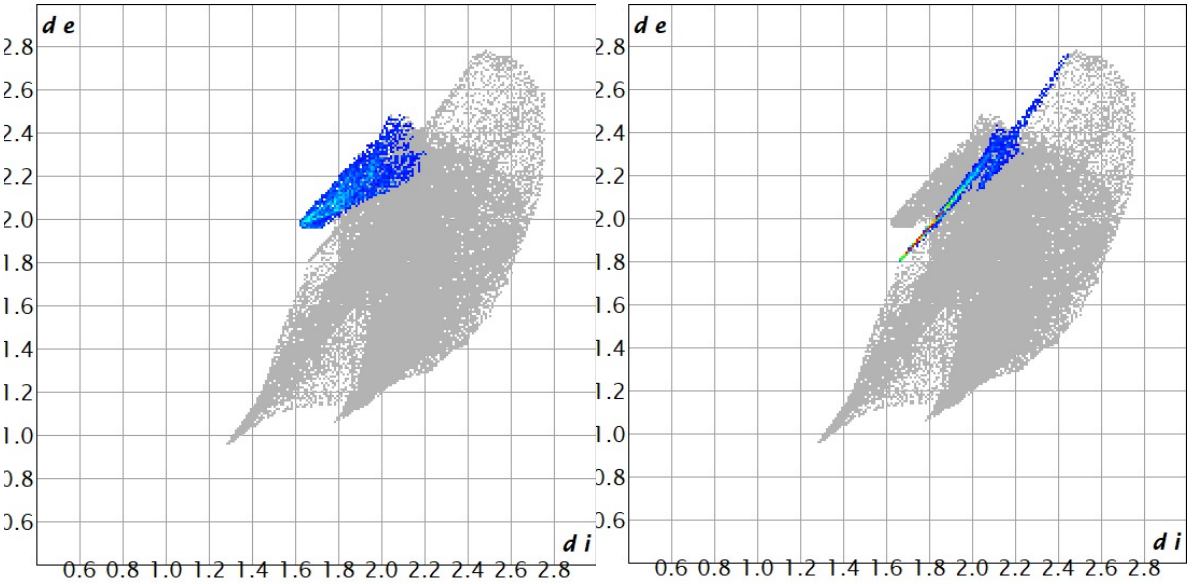

a) **b)**

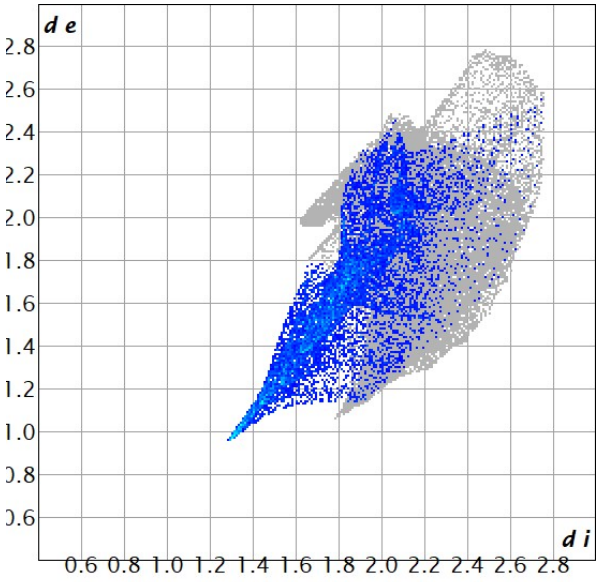

c)

Figure S14 Fingerprint plots of intermolecular contacts in **4** (at 100 K) for a) C···I, b) Br···I and c) O···H.

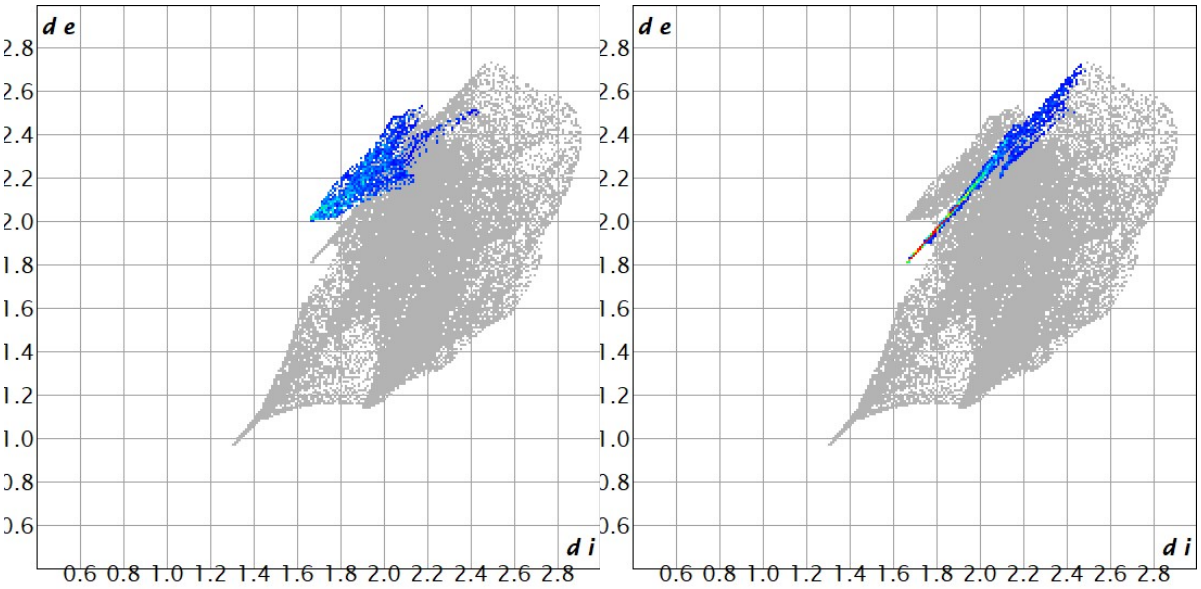

a) **b)**

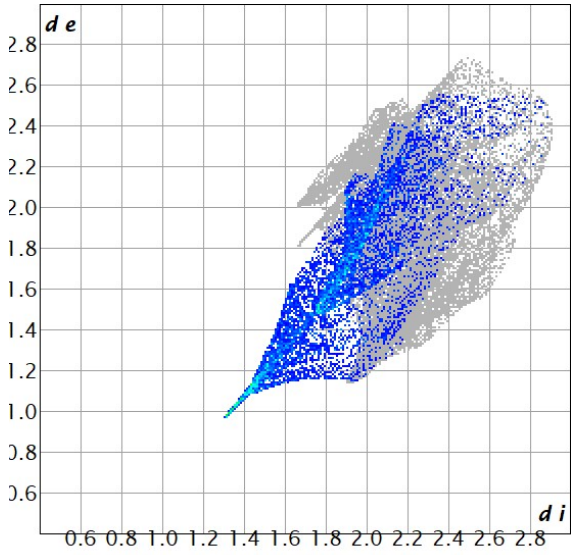

c)

Figure S15 Fingerprint plots of intermolecular contacts in **4** (at RT) for a) C···I, b) Br···I and c) O···H.

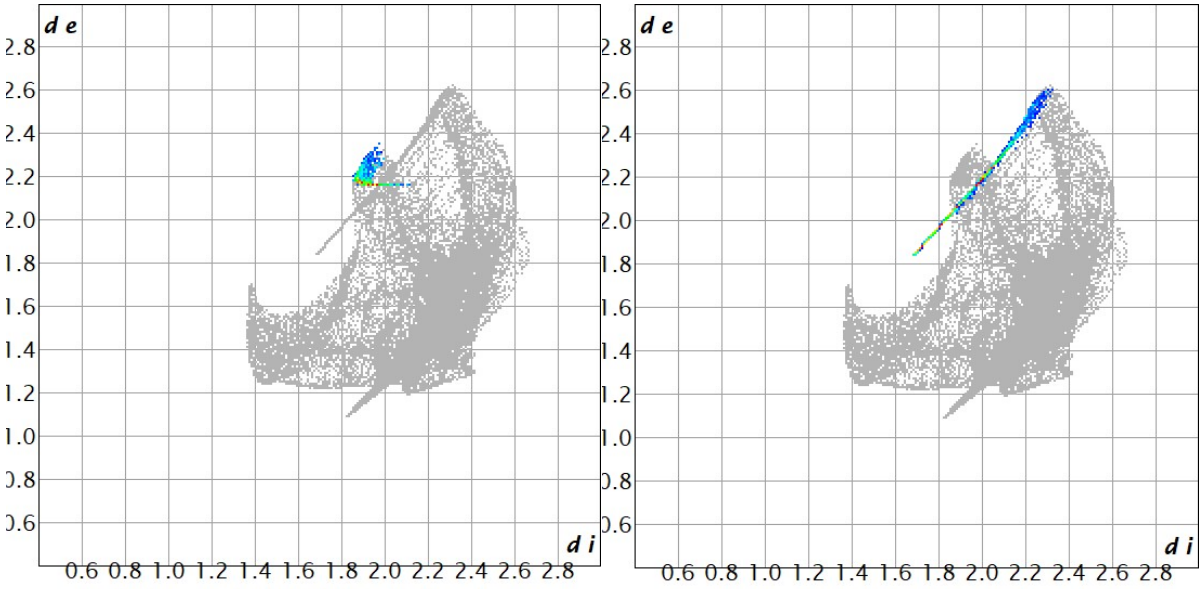

a) **b)**

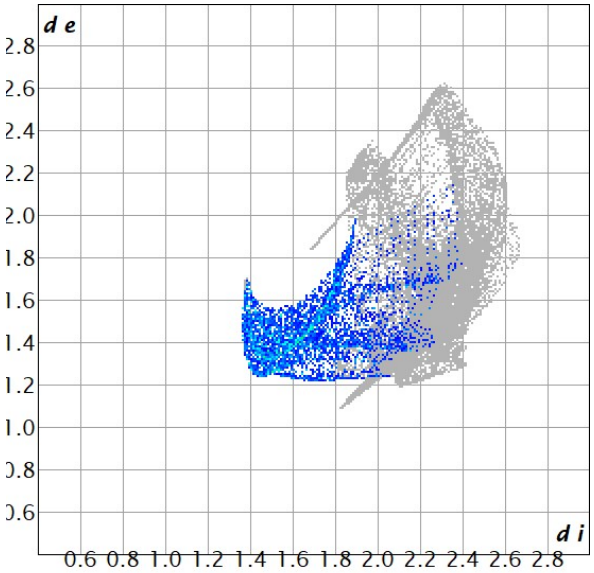

c)

Figure S16 Fingerprint plots of intermolecular contacts in **5** for a) C···I, b) Br···I and c) O···H.

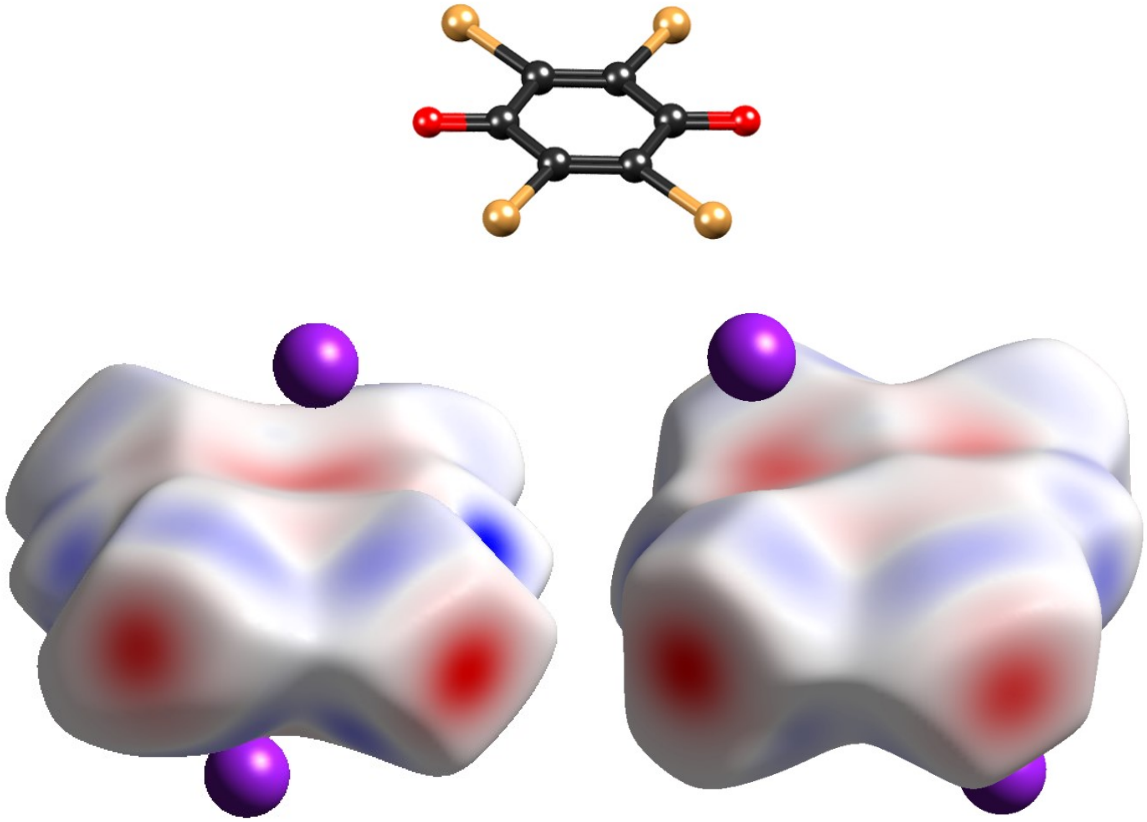

a) **b)**

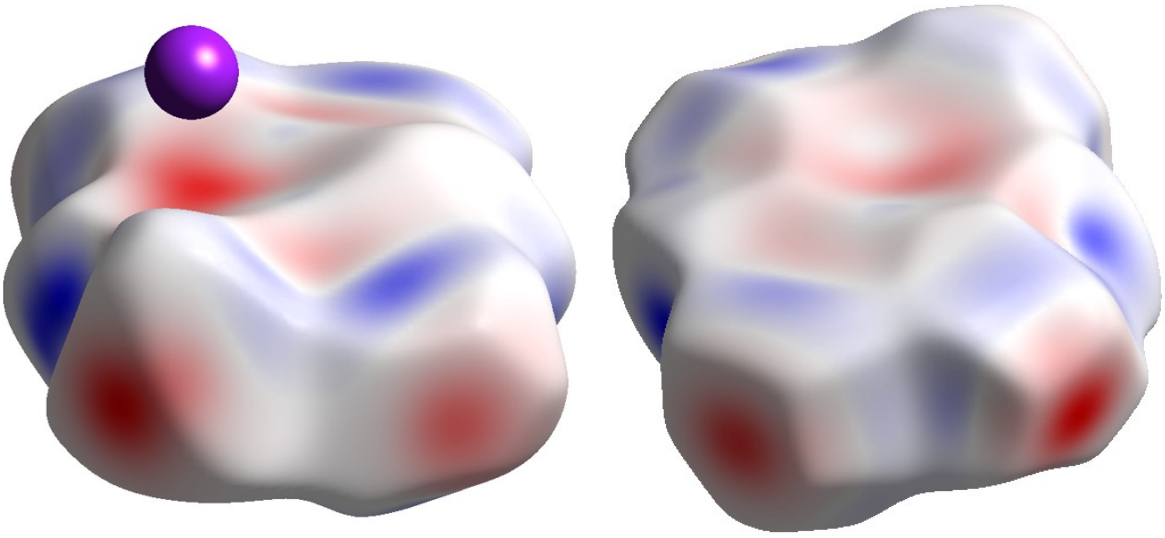

c)

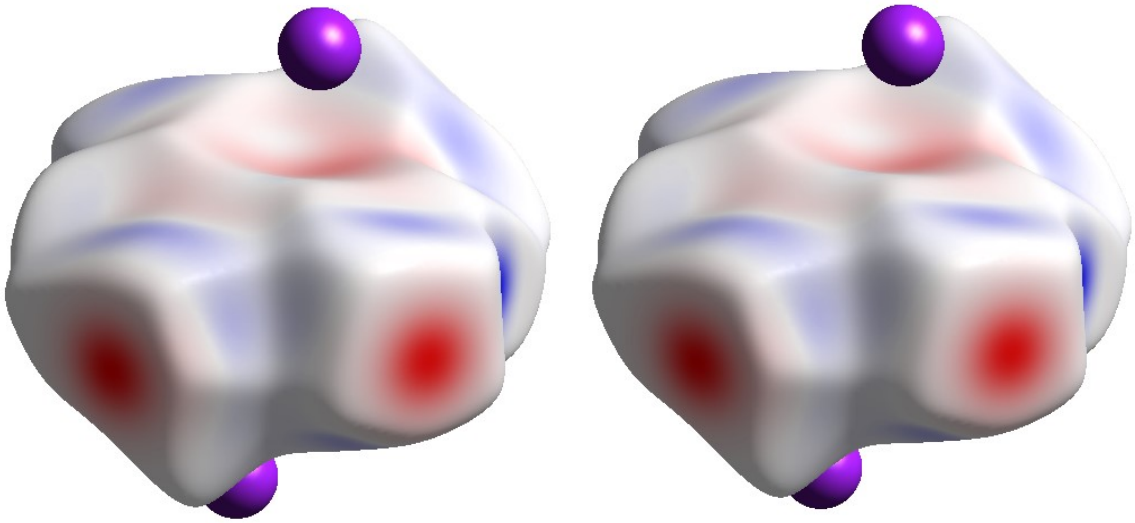

d) **e)**

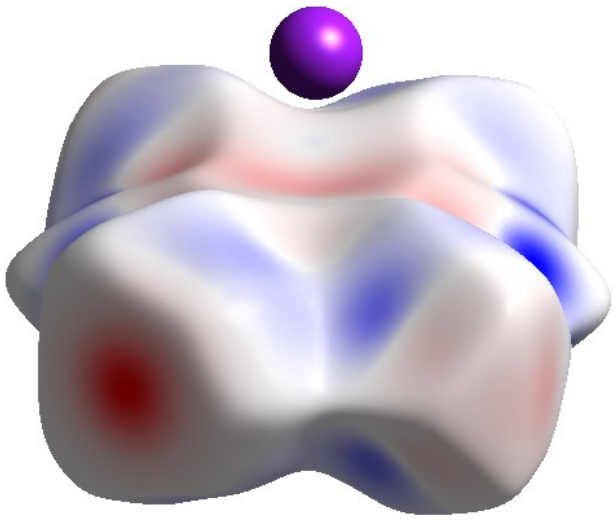

f)

Figure S17 Theoretical deformation electron density (computed by B3LYP/6-31G(d,p) method) plotted onto a Hirshfeld surface of Br_4Q for a) **1**, b) **2**, c) two symmetry-independent quinones in **3**, d) **4** at 100 K, e) **4** at RT and f) **5**. Positive density is shown in blue, and negative is red. Approximate orientation of the Br_4Q molecule is shown at the top.

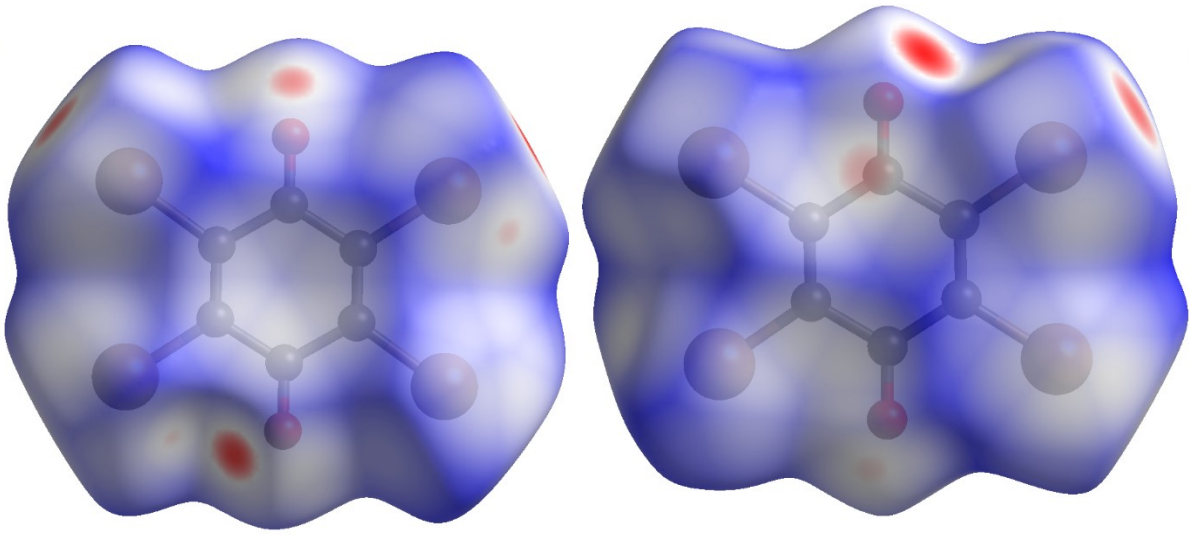

a) **b)**

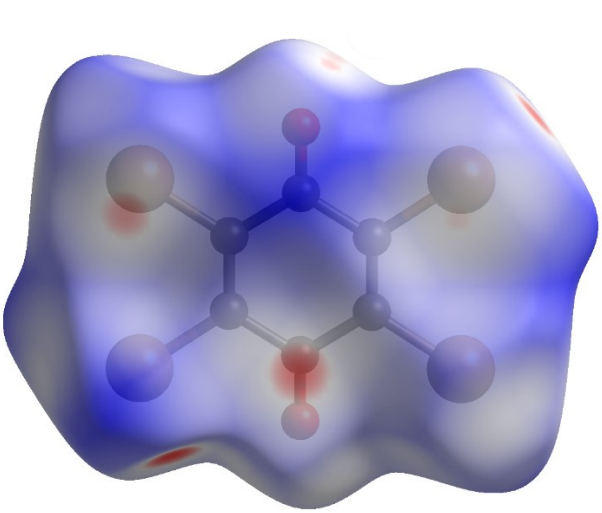

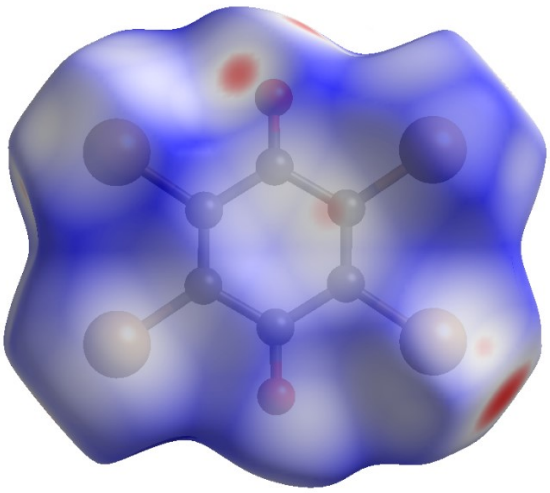

c)

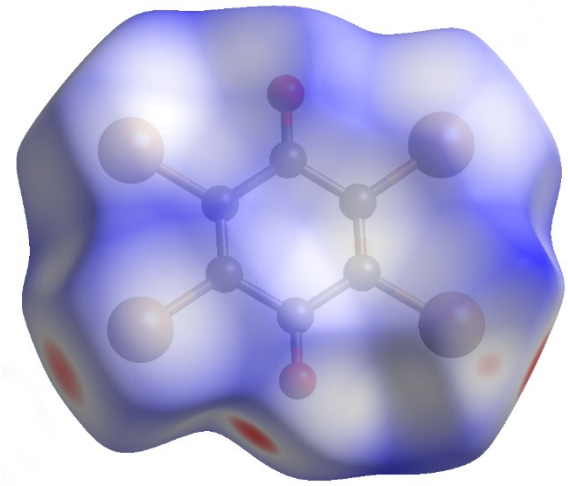

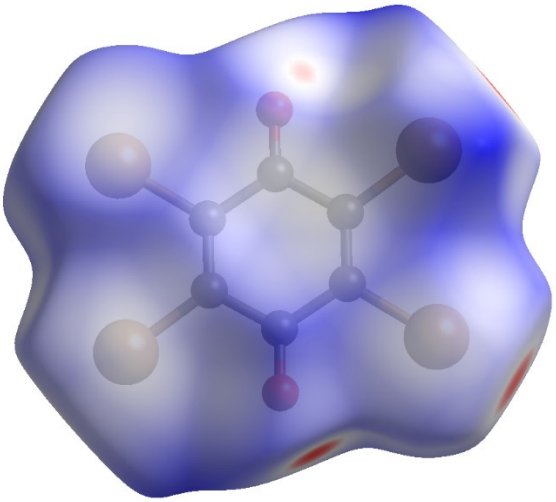

d) **e)**

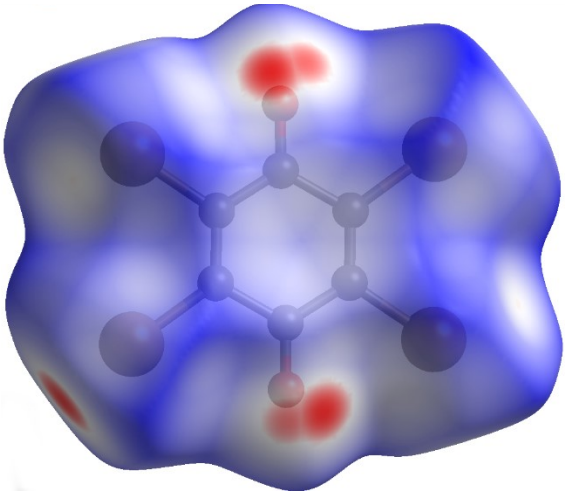

f)

Figure S18 Normalised distance (d_{norm}) plotted onto a Hirshfeld surface of Br_4Q for a) **1**, b) **2**, c) two symmetry-independent quinones in **3**, d) **4** at 100 K, e) **4** at RT and f) **5**. Red colour represents close contacts, while the more distant ones are shown in blue.

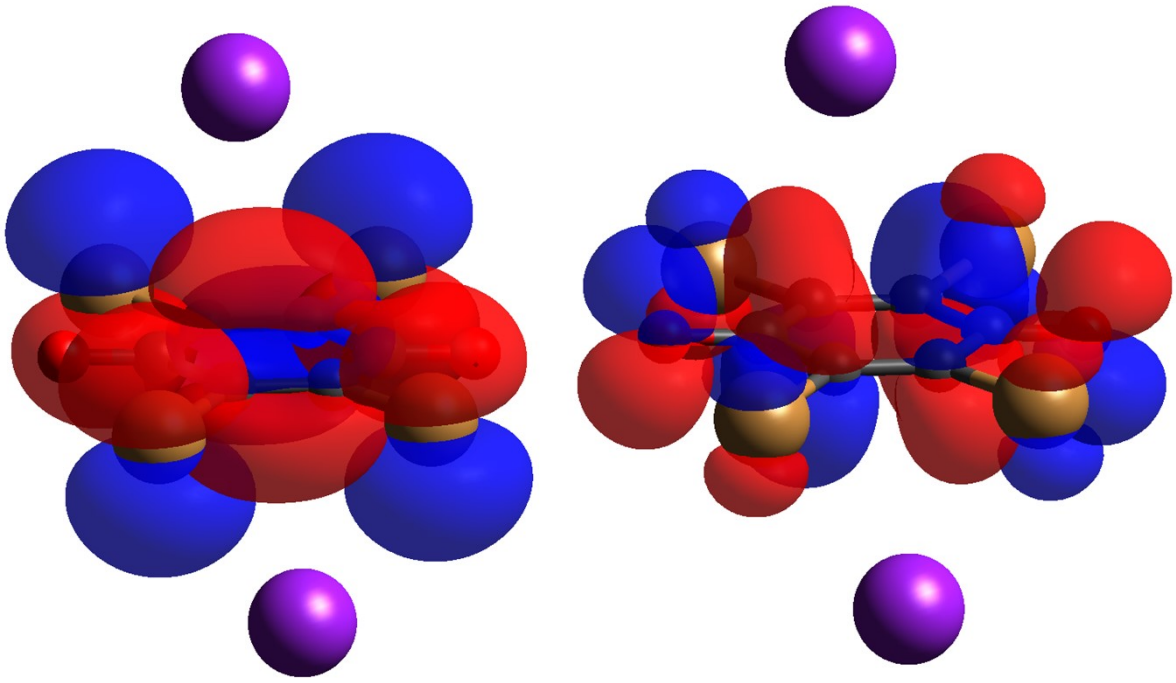

Figure S19 HOMO (left) and LUMO (right) orbitals of Br_4Q moiety in **1**. The orbitals were calculated using B3LYP method with 6-31G(d,p) basis set.

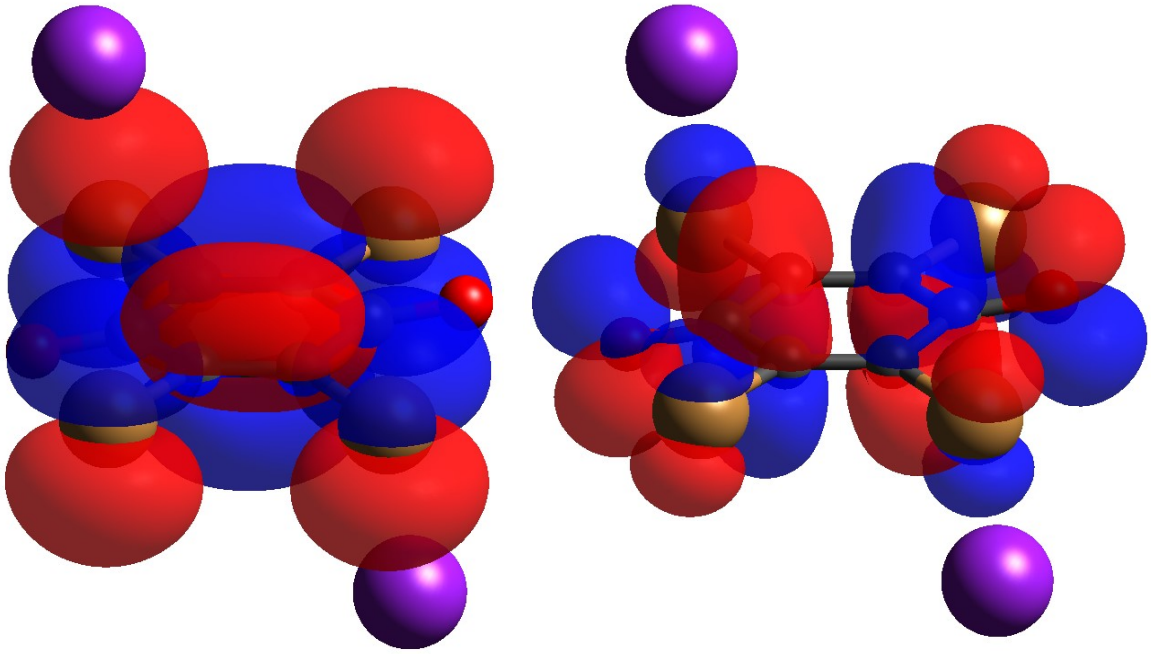

Figure S20 HOMO (left) and LUMO (right) orbitals of Br_4Q moiety in **2**. The orbitals were calculated using B3LYP method with 6-31G(d,p) basis set.

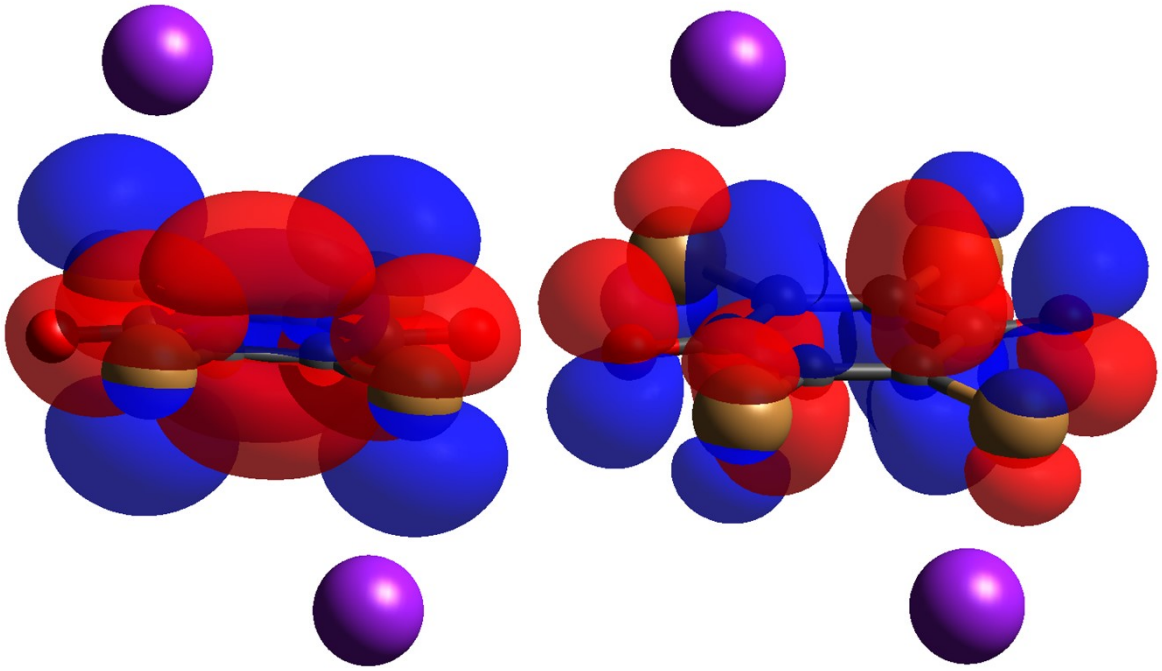

a)

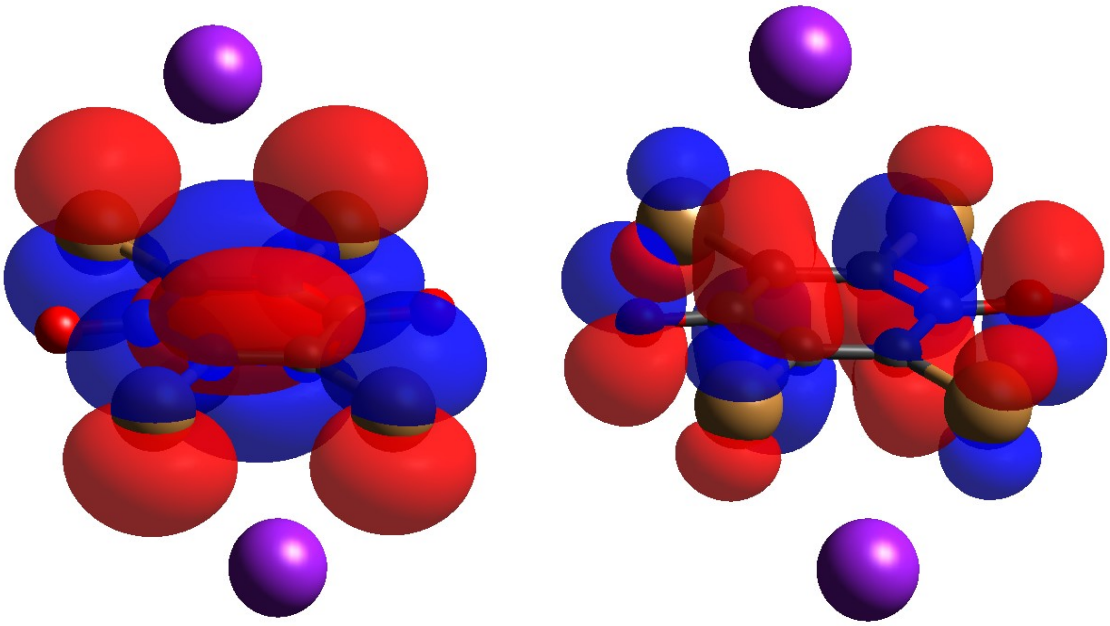

b)

Figure S21 HOMO (left) and LUMO (right) orbitals of Br_4Q moieties a) 1 and b) 2 in **3**. The orbitals were calculated using B3LYP method with 6-31G(d,p) basis set.

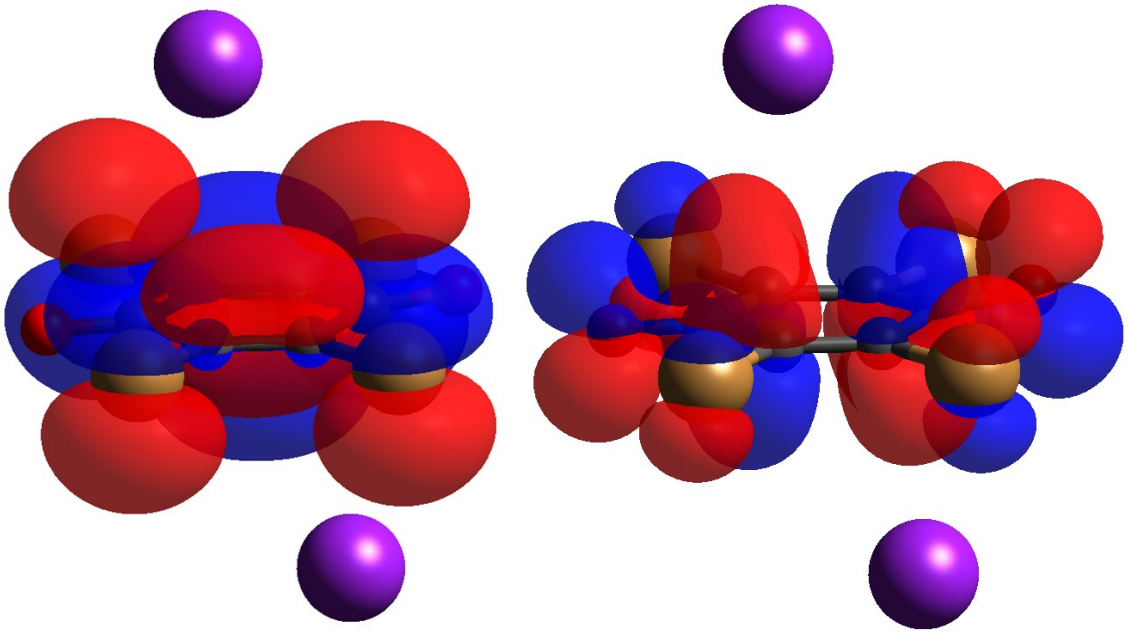

Figure S22 HOMO (left) and LUMO (right) orbitals of Br_4Q moiety in **4** at 100 K. The orbitals were calculated using B3LYP method with 6-31G(d,p) basis set.

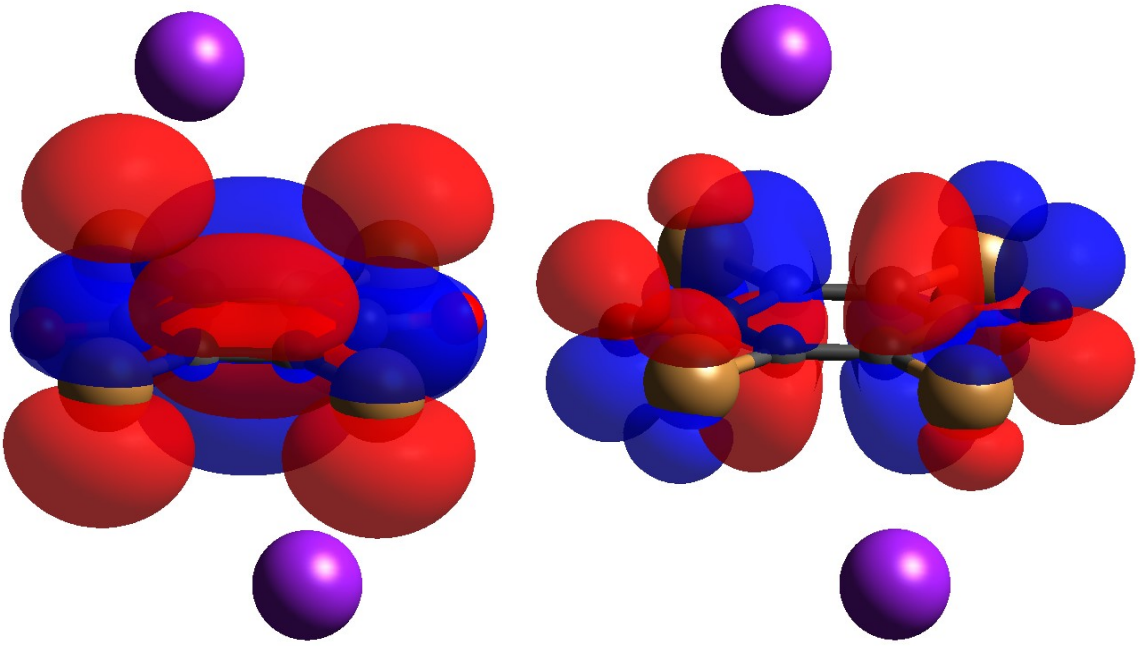

Figure S23 HOMO (left) and LUMO (right) orbitals of Br_4Q moiety in **4** at room temperature. The orbitals were calculated using B3LYP method with 6-31G(d,p) basis set.

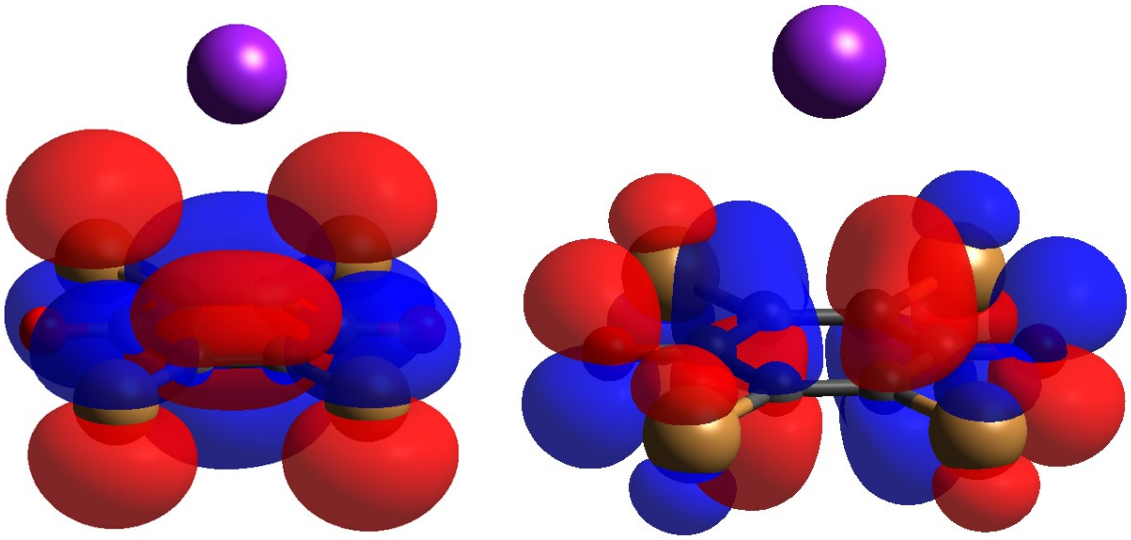

Figure S24 HOMO (left) and LUMO (right) orbitals of Br_4Q moiety in **5**. The orbitals were calculated using B3LYP method with 6-31G(d,p) basis set.

Table S1 Geometric parameters of hydrogen bonds (Å, °).

	D–H / Å	H···*A* / Å	*D*···*A* / Å	*D*–H···*A* / º	Symm. op. on *A*
1					
C4–H4···I2	0.93	2.35	3.617(9)	119	1–*x*, 1–*y*, 1–*z*
C9–H9B···I2	0.96	3.17	3.961(8)	140	3/2–*x*, –1/2+*y*, 1–*z*
C9–H9C···I2	0.96	3.09	3.922(9)	146	1–*x*, 1–*y*, 1–*z*
C10–H10···I2	0.93	2.98	3.886(8)	164	3/2–*x*, –1/2+*y*, 1–*z*
C14–H14···O1	0.93	2.49	3.310(12)	147	5/2–x, –1/2+y, 1–z
C15–H15A···I2	0.96	3.22	4.132(9)	159	3/2–*x*, –1/2+*y*, –*z*
C15–H15B···O1	0.96	2.79	3.304(11)	114	5/2–*x*, –1/2+*y*, 1–*z*
2					
C4–H4···I1	0.93	3.00	3.636(11)	127	1–*x*, 1–*y*, 1–*z*
C7–H7···I1	0.93	3.05	3.906(14)	154	1–*x*, –*y*, 1–*z*
C8–H8···O1	0.93	2.35	3.118(15)	140	2+*x*, *y*, 1+*z*
C9–H9A···O1	0.96	2.97	3.479(15)	114	2+*x*, *y*, 1+*z*
C9–H9A···I1	0.96	3.25	4.205(11)	171	1+*x*, *y*, 1+*z*
C9–H9B···Br2	0.96	3.07	3.925(12)	147	1–*x*, 1–*y*, 1–*z*
C10–H10B···O1	0.96	2.76	3.457(15)	130	2+*x*, *y*, 1+*z*
3					
N2–H2A···I1	0.86	3.03	3.860(5)	163	*x*, *y*, *z*
N2–H2B···I2	0.86	3.02	3.856(5)	166	–1+*x*, *y*, *z*
N4–H4A···I1	0.86	2.79	3.635(5)	167	*x*, *y*, *z*
N4–H4B···I2	0.86	2.85	3.666(6)	159	–1+*x*, *y*, *z*
C10–H10···O1	0.93	2.61	3.194(7)	121	1–*x*, 1–*y*, 1–*z*
C11–H11···O1	0.93	2.72	3.261(6)	118	1–*x*, 1–*y*, 1–*z*
C11–H11···Br1	0.93	2.81	3.601(6)	144	1–*x*, 1–*y*, 1–*z*
C14–H14···O2	0.93	2.56	3.354(7)	144	1–*x*, 1–*y*, 2–*z*
C17–H17···O2	0.93	2.61	3.084(7)	112	*x*, *y*, *z*
4, 100 K					
C7–H7···I1	0.93	3.20	3.727(10)	118	1–x, –1/2+*y*, 3/2–*z*
C8–H8···O1	0.93	2.42	3.248(11)	149	*x*, 1/2–*y*, –1/2+*z*
C9–H9···I1	0.93	3.06	3.981(10)	170	*x*, 1/2–*y*, –1/2+*z*
C11–H12B···I2	0.93	3.12	3.860(13)	138	–1+*x*, 3/2–*y*, –1/2+*z*
C12–H12B···I1	0.96	3.25	4.044(11)	141	1–x, –1/2+*y*, 3/2–*z*
C12–H12C···O1	0.96	2.65	3.284(12)	124	1–*x*, 1–*y*, 2–*z*
C14–H14···I2	0.93	3.19	3.925(13)	137	–1+*x*, –1+*y*, *z*
C16–H16···O2	0.93	2.39	3.249(18)	153	–1+*x*, –1+*y*, *z*
4, RT					
C4–H4···I1	0.94	3.06	3.926(13)	155	–*x*, 1–*y*, 1–*z*
C6–H6···I1	0.93	3.00	3.905(17)	164	*x*, *y*, *z*
C7–H7···O1	0.93	2.44	3.36(2)	169	1–*x*, 1–*y*, 1–*z*
C9–H9B···O1	0.96	2.61	3.367(18)	135	*x*, 3/2–*y*, 1/2+*z*
5					
C6–H6A···O1	0.96	2.92	3.060(16)	90	1–*x*, 1–*y*, –*z*
C6–H6B···O1	0.96	2.80	3.060(16)	96	1–*x*, 1–*y*, –*z*
C7–H7A···O1	0.96	2.69	2.963(17)	97	1–*x*, 1–*y*, –1+*z*
C7–H7B···O1	0.96	2.76	2.963(17)	92	1–*x*, 1–*y*, –1+*z*
C7–H7B···I2	0.96	3.23	4.065(12)	145	1+*x*, *y*, *z*

Table S2 Geometric parameters of π interactions in **3**.

$\pi\cdots\pi$	Cg[a]···Cg / Å	α[b]	β[c]	Cg···plane(Cg2) / Å	Offset/ Å	Symm. op. on Cg2
N1→C11···N1→C11	3.374(4)	0.0(3)	15.7	3.176(3)	0.916	1–*x*, –*y*, 1–*z*
N3→C17···N3→C17	3.556(4)	0.0(3)	13.0	3.465(3)	0.800	2–*x*, –*y*, 1–*z*
N3→C17···N3→C17	3.643(4)	0.0(3)	21.8	3.382(3)	1.354	1–*x*, 1–*y*, 2–*z*

[a] Cg = centre of gravity of the aromatic ring.

[b] α = angle between planes of two interacting rings.

[c] β = angle between Cg···Cg line and normal to the plane of the first interacting ring.

Crystal packing of compounds 2 - 4

3D packing of **2** is achieved by insertion of cations between I1···Br_4Q···I1 units (Fig. S25); there are three symmetry-independent halogen and seven hydrogen bonds (Tables 3 and S1).

In **3** planar cations form infinite stacks (Table S2) extending in the direction [100], and the I^-···quinone···I^- groups are located between these stacks (Fig. S26). There are two symmetry-independent stacks of cations and I^-···quinone···I^- groups. Due to the presence of strong proton-donating amino groups, hydrogen bonding is more extensive than in other structures. There are four symmetry-independent N–H···I hydrogen bonds, four C–H···O and one C–H···Br (Table S1); in addition, four C–Br···I halogen bonds link the I^-···quinone···I^- "sandwiches" (Table 3).

Crystal packing of two phases of **4** is the same, although in the low-temperature polymorph there is obviously lower symmetry (Fig. S27): cations are inserted between I^-···quinone···I^- units. Iodide anions accept two C–Br···I halogen bonds (Table 3), and there are weak hydrogen bonds with carbonyl oxygen atoms and iodide anions (Table S1).

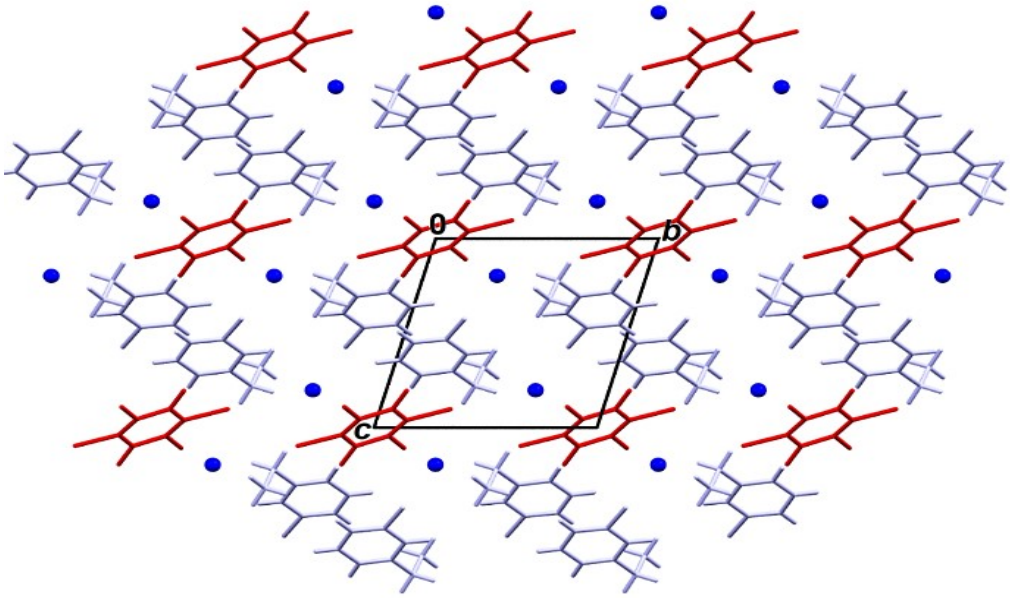

Figure S25 Crystal packing of **2**. Quinone molecules are shown red, iodide anions as blue and cations as pale purple. Iodide ions are shown as spheres of arbitrary radii.

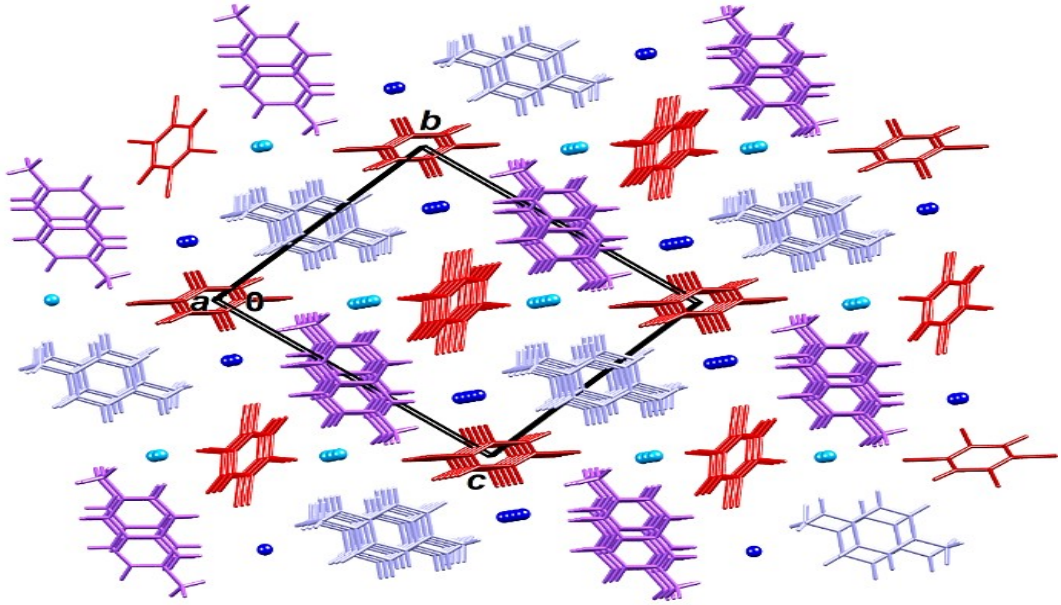

Figure S26 Crystal packing of **3**. Br_4Q molecules are shown as red (molecule 1 C1–C3 light red and molecule 2 C4–C6 as dark red), iodide anions are blue (I1 is dark blue, I2 is light blue) and two cations as purple (cation 1 N1–N2 dark purple, cation 2 N3–N4 pale

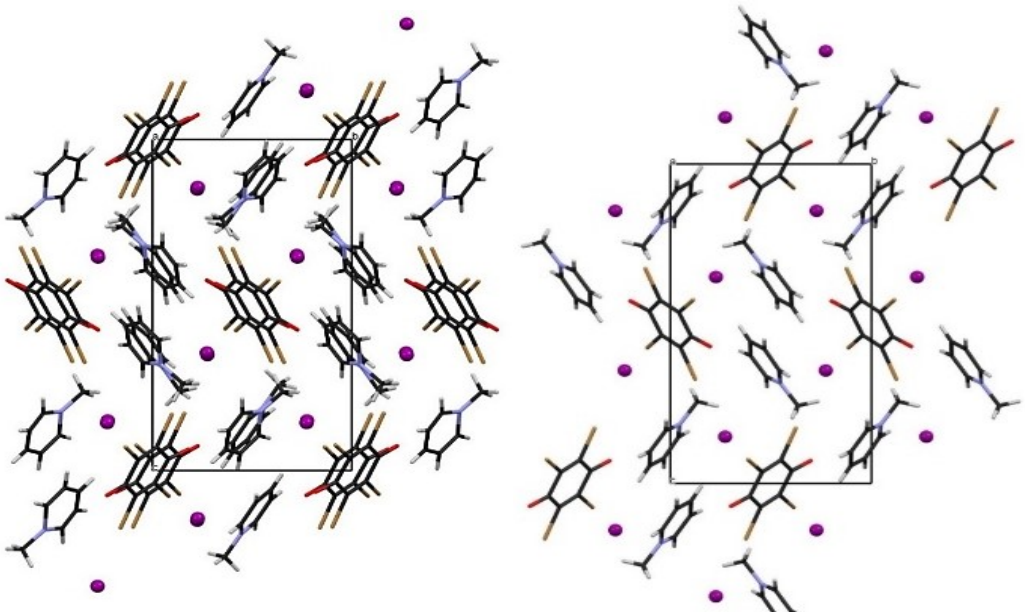

Figure S27 Crystal packing of **4**. Left: low-temperature phase (100 K), right: high-temperature phase (RT). Iodide ions are shown as spheres of arbitrary radii.

Table S3 Crystallographic, data collection and refinement data.

Compound	**1**	**2**	**3**	**4**	**4**	**5**
Empirical formula	$C_{15}H_{14}Br_2Cl_2I_2N_2O$	$C_{20}H_{18}Br_4Cl_2I_2N_2O_2$	$C_{18}H_{18}Br_4I_2N_4O_2$	$C_{18}H_{16}Br_4I_2N_2O_2$	$C_{18}H_{16}Br_4I_2N_2O_2$	$C_{20}H_{30}Br_4I_2N_4O_2$
Formula wt. / g mol^{-1}	722.80	962.70	895.76	865.77	865.77	931.88
Colour	black	black	black	black	black	black
Crystal dimensions / mm	0.15 x 0.15 x 0.15	0.25 x 0.08 x 0.06	0.10 x 0.07 x 0.05	0.22 x 0.08 x 0.07	0.18 x 0.08 x 0.07	0.20 x 0.06 x 0.03
Space group	$P\,2_1/a$	$P\,\bar{1}$	$P\,\bar{1}$	$P\,2_1/c$	$P\,2_1/c$	$P\,bam$
a / Å	10.9816(2)	8.5741(7)	7.0570(4)	15.4807(5)	7.7730(17)	13.9401(2)
b / Å	15.6952(2)	9.1611(7)	12.6851(6)	9.1376(4)	9.519(2)	13.8771(2)
c / Å	13.8514(2)	9.2506(7)	14.8883(9)	17.3524(5)	17.246(4)	7.60550(10)
α / °	90	105.323(7)	80.126(4)	90	90	90
β / °	110.729(2)	94.024(7)	77.986(5)	91.217(3)	91.254(4)	90
γ / °	90	95.605(7)	76.607(5)	90	90	90
Z	4	1	2	4	2	2
V / Å^3	2232.86(6)	693.94(10)	1257.45(13)	2454.05(15)	1276.0(5)	1471.27(4)
D_{calc} / g cm^{-3}	2.150	2.304	2.366	2.343	2.253	2.103
λ / Å	1.54179 (Cu$K\alpha$)	1.54179 (Cu$K\alpha$)	1.54179 (Cu$K\alpha$)	1.54179 (Cu$K\alpha$)	1.54179 (Cu$K\alpha$)	1.54179 (Cu$K\alpha$)
μ / mm^{-1}	28.571	26.493	27.282	27.902	26.831	23.499
Θ range / °	3.41 – 75.99	4.98 – 76.49	3.06 – 76.31	5.10 – 75.89	5.13 – 756	4.50 – 76.10
T / K	293(2)	293(1)	99(2)	100(2)	293(2)	293(2)
Diffractometer type	Xcalibur Nova	Xcalibur Nova	Xcalibur Nova	Xcalibur Nova	Xcalibur Nova	Xcalibur Nova
Range of h, k, l	$-11 < h < 13$; $-19 < k < 17$; $-15 < l < 17$	$-10 < h < 10$; $-11 < k < 7$; $-11 < l < 11$	$-8 < h < 8$; $-15 < k < 13$; $-18 < l < 18$	$-18 < h < 9$; $-9 < k < 11$; $-21 < l < 14$	$-9 < h < 9$; $-11 < k < 10$; $-14 < l < 20$	$-17 < h < 16$; $-17 < k < 17$; $-9 < l < 8$
Reflections collected	11894	5928	11628	13451	7004	13009
Independent reflections	4599	2857	5191	5063	2525	1651
Observed reflections ($I \geq 2\sigma$)	4397	2632	4916	4451	2305	1613
Absorption correction	Multi–scan	Multi–scan	Multi–scan	Multi–scan	Multi–scan	Multi–scan
T_{min}, T_{max}	0.3367; 1.0000	0.0593; 1.0000	0.3269; 1.0000	0.2052; 1.0000	0.3622; 1.0000	0.1039; 1.0000
R_{int}	0.0306	0.0573	0.0499	0.0544	0.0328	0.0471
R (F)	0.0522	0.0635	0.0507	0.0560	0.0579	0.0504
R_w (F^2)	0.1591	0.1949	0.1452	0.1565	0.1761	0.1660
Goodness of fit	1.048	1.099	0.928	1.044	1.037	1.163
H atom treatment	Constrained	Constrained	Constrained	Constrained	Constrained	Constrained
No. of parameters	217	145	273	94	127	94

No. of restraints	0	0	0	0	0	0
$\Delta\rho_{max}$, $\Delta\rho_{min}$ (eÅ^{-3})	2.611; –1.704	1.885; –1.931	1.635; –3.271	2.564; –2.280	1.815; –1.214	2.700; –0.786